Safety factor calibration for a new model of shear strength of reinforced concrete building beams and slabs

Jesús-Miguel Bairán[1], Joan R. Casas[2]

[1] *Associate Professor, Department of Civil and Environmental Engineering. Universitat Politècnica de Catalunya – BarcelonaTECH, Barcelona (Spain). Email: jesus.miguel.bairan@upc.edu*

[2] *Professor, Department of Civil and Environmental Engineering. Universitat Politècnica de Catalunya – BarcelonaTECH, Barcelona (Spain). Email: joan.ramon.casas@upc.edu*

ABSTRACT

When assessing existing structures, the availability of adequate safety factors, calibrated with the most accurate models, and for established target reliability indexes, is of critical importance in order to take the right decision regarding the maintenance/repair/strengthening interventions. In the case of shear resistance in reinforced concrete (RC) structures, when using the current design codes provisions for new constructions in assessment results that, in many cases, existing structures may be considered unsafe, implying large economic costs in strengthening or even dismantling. In this research, a proposal of safety factor relative to a recently developed model for shear strength, for elements with and without transversal reinforcement, based on a reliability-based calibration is presented. A formulation is proposed to determine the adequate strength factor for a selected target reliability index of the existing structure and desired remaining service life by means of a safety factor format, considering the load factors present in the Eurocodes. The calibration is carried out considering typical geometry and load ratios of building floors, as well as normal and high strength concrete. The derived safety factor is almost independent of the chosen remaining service life.

Keywords: safety factor; shear; reinforced concrete; assessment; reliability; building floors; beams, slabs

Bairan JM, Casas JR (2018), "Safety factor calibration for a new model of shear strength of reinforced concrete building beams and slabs", *Engineering Structures*, 172, 293-303. doi.org/10.1016/j.engstruct.2018.06.033

1. INTRODUCTION

The design process of a new concrete structure, or assessment of an existing one, should verify a limit-state condition of the form:

$$R_d \geq S_d \tag{1}$$

Being R_d and S_d the design values of the resistance and action-effects, respectively. The semi-probabilistic approach is the most common methodology used in practical applications. In this case, the action design value is computed by means of partial factors for loads, as e.g. Eq. (2) for the case of persistent or transient load situations. Here, $S_{G,ki}$ and $S_{Q,kj}$ are the characteristic values of the permanent action "i" and variable action "j", γ_{Gi} and γ_{Qj} are the partial safety factors for the permanent and variable actions. Variable load $j=1$ is the leading one, while the accompanying loads ($j>1$) are affected by a combination factor Ψ_j, which is less or equal to 1.0.

$$S_d = \sum_{i=1}^{n} \gamma_{Gi}\, S_{G,ki} + \gamma_{Q1} S_{Q,k1} + \sum_{j>1}^{n} \gamma_{Qj} \Psi_j\, S_{Q,kj} \tag{2}$$

The design value of the resistance may be computed by means of partial safety factors applied to materials characteristic values, usually concrete strength and steel yielding strength, as shown in Eq. (3), where f_{ck}, f_{yk}, γ_C, γ_S are the characteristic compressive strength, yielding strength and partial safety factors of concrete and steel. Alternatively, the design resistance can be obtained by a strength reduction factor, as shown in Eq. (4). In this case, γ_R is a strength safety factor which is applied in a global form to the resistance model, this is equivalent to the inverse of the strength reduction factor (ϕ).

In general, partial load factors account for the possibilities of unfavourable deviation of the load from its representative value, uncertainties in modelling of the load and of its effects. Materials partial factors and strength reduction factor account for the possibility of unfavourable deviation of the material property from the specified value, resisting model uncertainty, the geometrical deviations not considered explicitly and, in some cases, the consequences of failure.

Equations (3) and (4) represent, respectively, the two currently most used approaches in which safety factors are defined depending on the materials or the resisting mechanism involved, e.g. shear and bending require different strength reduction factors.

$$R_d = R\left(\frac{f_{ck}}{\gamma_C}; \frac{f_{yk}}{\gamma_S}\right) \tag{3}$$

$$R_d = \frac{1}{\gamma_R} R\left(f_{ck}; f_{yk}\right) = \frac{1}{\gamma_R} R_k = \phi R_k \tag{4}$$

If the partial safety factors have been appropriately calibrated, the required level of safety is deemed satisfied through the verification of Eq. (1). Strength reduction factors shall be used together with the same set of load factors considered in their calibration, in order to approach the target reliability. For example, in the 2002 version of ACI-318 [1], the load factors were modified to adapt them to the ASCE/SEI-7 [2] general provisions for minimum design loads in order to simplify the design process of structures with components of different materials, that required a recalibration of the strength reduction factor for shear, see Table 1. However, the alternative set of load and strength factors in Annex C of ACI-318 is allowed, if they are used together.

In ACI-318 the strength reduction factor also considers the brittle or ductile nature of the failure mode. As in the former, the element is more sensitive to larger variation of concrete strength in tension and compression and consequences of failure may be higher, hence a more conservative value of the resistance, i.e. a lower fractile, is needed to achieve the needed reliability.

Table 1: Load and strength safety factors in ACI-318 and Eurocodes

	ACI-318-02 [1]		Eurocodes [3, 4]
	Main body	Annex C (prior 2002)	
Dead load factor	1.2	1.4	1.35
Live load factor	1.6	1.7	1.5
Shear strength reduction factor ($\phi = 1/\gamma_R$)	0.75	0.85	-
Concrete strength partial safety factor (γ_C)	-	-	1.5
Steel strength partial safety factor (γ_S)	-	-	1.15

On the other hand, Eurocodes 2 [3] and 1 [4] provide a set of partial safety factors for steel (γ_S) and concrete (γ_C) properties, together with a set of partial load factors. The code was calibrated for a yearly target reliability index of $\beta_1 = 4.7$, which is equivalent to a nominal probability of failure in 1 year of approximately 10^{-6} [5].

When dealing with the assessment and/or strengthening of an existing building, a question about the suitability of using the same partial safety factors of the design of new elements arises. In general, there is less uncertainty in the geometrical and material parameters and an increment of the safety level may require a much larger economic effort than to achieve the same increment in a new design. Additionally, the required remaining service life may be shorter than in new constructions.

Therefore, the definition of the target reliability level for assessing existing structures should be based on risk of failure and cost optimization; including repair interventions, losses due to malfunction, environmental and psychological effects. A framework for establishing the target reliability corresponding to a remaining service life is available in some codes, as ISO 13822 [6], ISO 2394 [7], and recommendations, such as fib [8]. Hence, economic optimization can be used to derive target reliability values. However, human safety levels based on individual and societal risk for ethical issues should also be considered in the process, as stated in Sýkora et al. [9], Tanner and Hingorani [10], Steenbergen et al. [11]. As concluded in Steenbergen et al. [11], the minimum levels related to human safety are often critical target reliabilities for existing structures.

After the target reliability index is defined, suitable and properly calibrated resistance models are needed, including the statistical definition of the model error. The particular case of assessing shear resistance in existing concrete elements has gained much attention recently, as the current design provisions have raised doubts regarding the safety of constructed facilities, implying that many structures are to be strengthened or dismantled. Furthermore, contrary to bending strength, whose resisting theory is well consolidated, there are currently several shear strength theories, based on different hypotheses and with different accuracy and complexity levels. In recent investigations, experimental tests have been conducted in existing structures or elements that were deemed unsafe according to current design provisions, e.g. Zwicky and Vögel [12], Bergström et al. [13]. In some cases, shear performance observed by experimentation was much better than the expected according to the provisions for new structures. The use of adequate non-linear computational models accounting for non-linear shear behavior have also shown similar results, Ferreira et al. [14, 15]. Hence, it can be expected certain cost reduction in strengthening of structures or even no need of posting or substitution, after an advanced assessment of the existing safety level.

However, adequate nonlinear models for shear assessment are not always available, or it is not possible to systematically build a computational model for a large number of different structures in a network and perform the probabilistic analyses. Therefore, simpler models that are adequate for hand or spreadsheet calculations are useful in these cases. In addition, for practical and fast assessment application in a semi-probabilistic format, the strength reduction factors should be calibrated.

The objective of the present study is to propose adequate reliability-based design/assessment equations with properly calibrated safety factors for reinforced concrete beams and slabs of buildings, failing in shear, for a various target reliability indexes. The current method is restricted to shear failure taking place in sections that have not yielded previously in bending or axial force.

The paper is organized in the following way. Section 2 presents a statistical analysis of selected existing models for shear resistance in concrete members to define the most accurate and statistically define the corresponding model error. By the use of this model and after the definition of the sample set, Section 3 carries out the calibration process to define the safety factor, and the analysis of the results and discussion is presented in Section 4. Finally, the main conclusions are drawn in Section 5.

2. SHEAR RESISTANCE MODEL

For an appropriate calibration of safety factors, the first step is to derive accurate design equations for the shear strength capacity of reinforced concrete beams, based on the available theoretical models, jointly with the statistical characterization of the random variable of the "model error". This random variable represents the ratio of the actual response to the model prediction and is characterized by a statistical distribution, its mean value (or bias ratio) and standard deviation (or coefficient of variation, CoV).

In this paper, a recently mechanical-based formulation for shear-flexure strength of reinforced concrete beams, proposed in Mari et al. [16], is used. This model assumes a combination of the four classical shear resisting mechanisms; namely, capacity of the uncracked compression chord (V_c), capacity of the diagonally cracked web (V_w) and the contribution of the transverse (V_s) and longitudinal reinforcements (V_l). The model provides a set of mechanistic derived closed-form equations for each action, here summarized in Table 2.

2.1. DESCRIPTION

The main aspects of the model can be explained based on Fig. 1; here, the shear stress distributions in a reinforced concrete beam are analyzed for the free-body equilibrium of the segment of the beam between the cross-sections 1 and 2 (Fig. 1a), at the initiation of an inclined crack in the tensile side and its tip, respectively. As discussed in Marí et al. [16] and Bairán and Marí [17, 18], the distribution of shear stresses depends on the crack pattern and bond between concrete and reinforcement. Fig. 1b shows the shear stress distribution for an almost vertical crack and perfect bond between reinforcement and concrete, the stresses are almost constant in the tensile cracked portion and corresponds to the so-called *beam-action*. Although acceptable in wide range of load stages, these hypotheses do not hold up to failure and thus shear stress distribution varies.

In the ideal situation of zero bond of the longitudinal reinforcement, its tensile force is constant between the two sections and the stress distribution is as in Fig. 1c, with a variation of the lever arm. This leads to a pure *arch-action* in which shear stresses are resisted only in the compression chord. Although completely loss of bond is not likely if ribbed reinforcement with adequate development length is used, bond deterioration takes place as shear damage propagates. Recently, Carmona and Ruiz [19] studied the role of bond deterioration on shear resistance on the basis of fracture mechanics and Yang [20] related the formation of the longitudinal crack at the level of tensile reinforcement with the on-set of shear failure. Therefore, it is plausible to accept that bond will develop imperfect during the evolution of shear resisting actions.

In the cracked portion of the beam, shear stresses can be resisted by aggregate interlock, residual tensile stresses and inclined compression stress field. However, after crack opening increases, it is considered that the residual tensile stresses concentrate in the portion close to the neutral axis, where crack width is still moderate, and in the uncracked compression chord; while in the region with larger crack width, mainly the inclined compression strut acts. In this situation, the distribution of shear stresses is depicted in Fig. 1d. The variation of tensile force is less than for perfect beam-action and a combination of normal and shear stresses exist in the uncracked compression chord. This is an intermediate situation between the perfect *beam-action* (Fig. 1b) and the perfect *arch-action* (Fig. 1c). The compression stresses in the shear cracked portion of the beam result from the longitudinal component of the inclined compression field.

The model was developed for elements that fail in shear before yielding of the longitudinal reinforcement, so longitudinal reinforcement is elastic and the normal stresses in the compression zone is considered to follow a linear distribution. The main hypothesis of the model is that, as shear cracking opens and evolves, the distribution of shear stresses in the critical region varies from one similar to Fig. 1b to that of Fig. 1d, making the magnitude of shear stresses in the compression head to increase. The details on the derivation of the model equations can be found in [16]; however, in the following, a global description of the process is presented.

Firstly, the shear contribution of the cracked web (v_w) is estimated from the residual tensile strength according to the concrete's tensile fracture energy and the maximum crack width; which is computed from the tensile strain in the longitudinal bar and by approximating the crack spacing by the element's depth. The tensile force resulting from the integration of the previous stresses is taken orthogonal to the crack's inclination and its vertical component is the shear contribution of the web.

On the other hand, in the presence of transversal reinforcement, its contribution to shear strength is the summation of all tensile ties crossed by the inclined crack (v_s). Also, if transversal reinforcement exists; the contribution of longitudinal reinforcement (dowel action) is taken into account (v_l). In order to compute the previous components, the inclination of the shear crack is needed. In the shear critical region, the crack inclination is estimated after Eq. (5). In this equation, *x/d* is the ratio of the neutral axis with linear stress distribution and the effective depth.

$$\cot\theta = \frac{0.85}{1-\frac{x}{d}} \tag{5}$$

The shear force that must be resisted by the compression zone is computed from equilibrium by subtracting the three previous components (V_w, V_l, V_s) from the applied shear force, Eq. (6).

$$V_c = V_{Ed} - V_w - V_l - V_s \tag{6}$$

To determine the shear capacity of the compression chord, the normal and shear forces are distributed according to an elastic hypothesis. In the presence of closed hoops as transversal reinforcement, the confining stresses in in the compression chord is accounted for. Further, the tension and compression principal stresses can be computed along the compression chord.

Shear failure is assumed to occur when the most critical point in the compression chord reaches its maximum capacity defined by the failure surface proposed by Kupfer et al. [21], see Fig. 2; otherwise, the element resists the applied load. In Fig. 2, it is represented the elastic limit observed in [21], where the Elastic Modulus and Poisson coefficient of concrete starts to vary from the initial one. The volumetric expansion is the situation prior to failure where concrete lateral expansion starts. It can be observed that in the compression-tension region, the volumetric expansion and strength envelope practically coincide. Therefore, in the model, the linear distribution of compression stresses is considered in the compression chord. Moreover, the capacity of this resistance mechanism depends on both compression and tension strengths.

In order to find the maximum shear strength, an iteration is needed in which the applied load (V_{Ed}) is increased until a point in Kupfer's failure surface is found. This process is rather tedious for practical purposes, so a parametric study was carried out that showed that the solution to the compression head contribution could be approximated by a linear relationship (Fig. 3), resulting in Eq. (7).

The linearized model is summarized in Table 2, where all terms have been normalized by $f_{ct}bd$. Note that here, the tensile strength is the reference parameter, in contrast to other formulations that are based on compression strength. The additional symbols in the equations of Table 2 are defined in Eqs. (11) to (15).

The factor ζ represents the size effect of the shear capacity of the compression chord, which was taken similar to the proposal of [22], which was based on experimental observation on beams without shear reinforcement, Eq. 11. The term "a" is the shear span, given by Eq. (12). It should be noticed that, in this model, a is computed on the basis of the maximum absolute bending moment and shear forces in the region of the beam under consideration up to the point of zero moment. Fig. 4 shows how to compute the shear span in the different regions of a beam.

For rectangular sections, x/d can be computed from Eq. (13), with α_e being the ratio of elastic modules of steel to concrete, Eq. (14). G_f is the fracture energy in Mode I of tension. In case it cannot be measured experimentally, Eq. (15) was proposed in [16] as a modification of the equation of Model Code [23] to account for the effect of the aggregate size (d_{max}).

Table 2. Summary of simplified equations derived for the different shear contributing actions

Compression chord	$v_c = \frac{V_c}{f_{ct}bd} = \zeta\left[(0.88 + 0.70v_s)\frac{x}{d} + 0.02\right]$	(7)
Cracked concrete web	$v_w = \frac{V_w}{f_{ct}bd} = 167\frac{f_{ct}}{E_c}\left(1 + \frac{2E_cG_f}{{f_{ct}}^2 d}\right)$	(8)
Longitudinal reinforcement	$v_s > 0 \rightarrow v_l = \frac{V_l}{f_{ct}bd} = 0.25\frac{x}{d} - 0.05$	(9a)
	$v_s = 0 \rightarrow v_l = 0$	(9b)
Transversal reinforcement	$v_s = \frac{V_s}{f_{ct}bd} = 0.85\rho_w\frac{f_{yw}}{f_{ct}}$	(10)

$$\zeta = 1.2 - 0.2a \geq 0.65 \tag{11}$$

$$a = \frac{|M_{max,shear\ span}|}{|V_{max,shear\ span}|} \tag{12}$$

$$\frac{x}{d} = \alpha_e\,\rho\left(-1 + \sqrt{1 + \frac{2}{\alpha_e\,\rho}}\right) \tag{13}$$

$$\alpha_e = \frac{E_s}{E_c} \tag{14}$$

$$G_f = 0.028 f_{cm}^{0.18} d_{max}^{0.32} \tag{15}$$

This model accounts for the failure mode of tension failure produced by shear forces. Two additional failure modes should be verified for the sake of completeness of the shear assessment. First, the failure of the diagonal compression stresses in the cracked web, which can be computed after Eq. (16) [3], by considering the inclination of the compression field from Eq. (5). Second, the capacity of the longitudinal reinforcement to resist the tensile force produced by the bending and axial force together with the increment produced by shear given in Eq. (17).

$$V_{Rd,max} = \alpha_{cw} b_w z \nu_1 f_{cd} \frac{1}{\cot\theta + \tan\theta} \tag{16}$$

$$\Delta F_t = (V_{Ed} - 0.5V_s)\cot\theta \quad (17)$$

2.2. MODEL ERROR

The model error was estimated by comparing the prediction against experimental databases collected in [24], [25] and [26], for elements with and without transversal reinforcement, as presented in [16]. The database included the reported average values of compression strength and yielding strength of the reinforcements. The concrete tensile strength was estimated from compression strength using [3], see Table 5. The model error was also compared against those of Eurocode 2 [3], ACI-318 [1] and Model Code 2010 [23]. The error characteristics of these models correspond well with those recently found in [27]. As can be seen in Table 3, the above model shows better performance in terms of average and CoV of the model error for both situations, which makes it a good option for an assessment model.

Table 3. Statistical characterization of the error of different shear resisting models

	892 beams without transversal reinforcement				239 beams with transversal reinforcement			
V_{test}/V_{pred}	EC-2	ACI 318-08	MC10 Lev II	Model. [16]	EC-2	ACI 318-08	MC10 Lev III	Model [16]
Average	1.07	1.28	1.20	1.04	1.72	1.25	1.21	1.02
Standard Deviation	0.226	0.346	0.223	0.179	0.638	0.262	0.225	0.169
CoV	0.211	0.271	0.186	0.173	0.371	0.210	0.186	0.166

3. SAFETY FACTOR CALIBRATION

The design equation (18) is selected, with a safety factor γ_R. $V_{R,k}$ is the shear strength computed according to Section 2, using the characteristic material properties for concrete tensile strength, Eq. (19).

$$\frac{1}{\gamma_R} V_{R,k} \geq \sum_i \gamma_{G,i} V_{G,ki} + \gamma_{Q,1} V_{Q,k1} + \sum_{j>1} \gamma_{Q,j} \Psi_j V_{Q,kj} \quad (18)$$

$$V_{R,k} = (v_c + v_w + v_l + v_s) f_{ct,k} bd \quad (19)$$

$V_{G,ki}$ is the shear force produced by the characteristic value of the dead load i, and $\gamma_{G,i}$ is the partial safety factor of the dead load i. $V_{Q,,k1}$ is the shear force due to the characteristic value of the leading service load and $V_{Q,,kj}$ is the shear force due to the accompanying load acting in combination with the leading one. $\gamma_{Q,j}$ is the partial safety factor for load j and Ψ_j the combination factor for the accompanying load. In this study, the Eurocode partial factors for actions of Table 1 were used. The characteristic design loads and characteristic material properties were selected according to Eurocode 1 and 2 [4, 3].

The next step is to specify the range of possible structures/elements where the obtained safety factors will be of application.

3.1. BUILDING FLOOR DESIGN SET

In order to determine the geometric characteristic and applied loads, a reference design set of typical floors was created, considering different values of beam length (l) and distance between adjacent beams (s). The combination of values for geometry and material strength in the design set are described in Table 4, producing 108 design cases. Here, *h* and *b* are the depth and width of the rectangular beam (see Fig. 5).

Table 4. Range of variables in the design set

Variable	Values	Nº cases
l (m)	4, 8, 12	3
s (m)	3, 6, 9	3
l/h (-)	10, 15, 20	3
b/h (-)	0.5	1
f_{ck} (MPa)	25, 50, 70, 90	4
	Total Nº cases considered:	108

As described in Section 2.1, in this model, the size effect of V_c depends on the shear span (*a*). Without losing generality, all elements are considered as simply supported. In this case, *a* can be computed as shown in Fig. 5; hence, *a* is uniformly distributed between 1 m and 3 m.

It should be noticed that the shear span ratio (*a*/d) is known to affect the shear resistance through both moment-shear interaction and size effect [22]. As shown in [16], if the shear failure takes place without yielding of the longitudinal reinforcement, the most critical section in shear results to be the one in the tip of the crack closest to the point of zero bending. Therefore, the effect of accompanying bending moment interaction was conservatively accounted for by assuming it as the cracking moment.

On the other hand, the number of tests with distributed loads is scant with respect to those with point loads. However, it has been observed that the elements with distributed loads tend to have higher resistance than the equivalent specimen with point loads, [28], [29], among others. The effect of distributed loads in the current model was discussed in [30]. It was observed that the critical shear crack tend to occur closer to the zero-moment section and, on the other, the maximum reaction can be estimated by adding the resultant of the distributed load from the tip of inclined crack to the support.

The resulting distribution of live to dead load ratio (L/D) is shown in Fig. 6. L/D in the set ranges between 0.29 and 0.80, with a mean value of 0.60. It should be noticed that the difference with respect to the range considered in Ellingwood et al [31] (0.25 to 1.5) is justified because Ellingwood et al considered the wider range of live loads in the Building Code (including stage floors), while here the calibration is made for office and residential use. When considering office loads in [31], the range of L/D ratio is consistent with the here used.

To avoid bending failure in the representative set of beams the longitudinal reinforcement was over-designed in bending by a factor of 1.5. The shear reinforcement ratio ($\rho_w f_{yd}$) that would result from the application of current Eurocode provisions in this design set ranges between 0 and 8.8 MPa, with an average value of 1.17 MPa. 90% of the specimens in the set would require $\rho_w f_{yd} \leq 3$ MPa, and the lower 60% of the set will require $\rho_w f_{yd} \leq 1$ MPa, which makes it consistent with the usual reinforcement ratio used in this kind of structures.

3.2 CALIBRATION

The shear resistance safety factor (γ_R) in Eq. (18) is calibrated based on the selection of a uniform reliability index (the target value) for the design set; as applied by several authors, e.g. Melchers [32], Madsen et al. [33], Casas [34], Casas and Chambi [35], Trentin and Casas [36], among others. Accordingly, when using the design equation (18), it should yield almost uniform reliability indexes close to the target value (β^*).

In general, the shear resistance for the trial value of γ_R is first computed assuming vs=0; if the resistence is bigger than the design shear force, then no shear reinforcement is needed. Otherwise, shear reinforcement is designed. Afterwards, the reliability index of each designed case is computed by means of FORM (*First-Order Reliability Method)* analysis, with the limit state function defined in Eq. (20). Here, V_R is the random variable representing the shear resistance computed as function of the random variables of Table 5, as shown in Eq. (21).

Table 5. Basic random variables in the resistance term (V_R)

Variable	Description	Statistical model	μ	CoV	Ref.
δ	Model error	Log-normal	ρ_w=0: 1.04 ρ_w >0: 1.02	0.173 0.166	Table 3
f_c	Concrete compression strength	Log-normal	f_{ck}+8MPa	0.05 – 0.147	[3, 37]
f_{ct}	Concrete tensile strength	Log-normal	$f_{ctm} = 0.3 f_{ck}^{\frac{2}{3}}$ $for\ f_{ck} \leq 50\ MPa$ $f_{ctm} = 2.12\ \ln\left(1 + \frac{f_{cm}}{10}\right)$ $for\ f_{ck} > 50\ MPa$	0.182	[3, 37]
f_y	Reinforcement yielding stress	Log-normal	550 MPa	0.055	[37]
Δb	Geometrical error in section's width	Normal	$0.003b \leq 3mm$	$\frac{4 + 0.006b \leq 10mm}{\mu_b}$	[37]
Δd	Geometrical error in section's effective depth	Normal	$10\ mm$	1	[37]

$$G = V_R - V_E \tag{20}$$

$$V_R = \delta \cdot V_{R,mod}(f_c, f_{ct}, f_y, b + \Delta b, d + \Delta d, A_s, A'_s) \tag{21}$$

A random variable (δ) is considered in Eq. (21) to take into account the model error. According to the recommendations of JCSS [37], δ is set as Log-Normal; its parameters were selected according to the results of Table 3. The parameters of δ are defined in Table 5 for elements without shear reinforcement (ρ_w=0) and with shear reinforcement (ρ_w>0).

V_E is the shear force in the critical section, which is a function of the load random variables of Table 6. These variables may be considered as uncorrelated because they are due to independent actions (self-weight, permanent load, live-load, etc.). The nominal value for the self-weight load is calculated based on the dimensions of the elements and the density of reinforced concrete.

Following the recommendations in [37], the live load model is taken, as a Gamma distribution for the sustained load, with mean and standard deviation μ_q and σ_q, respectively. Variations in time of the sustained load is further taken into account by assuming that the time between load changes is exponentially distributed. Therefore, the probability function for the maximum sustained load is given by Eq. (22).

Table 6. Basic random variables in the action term (V_E)

Variable	Description	Statistical model	μ	CoV	λ	T	Ref.
g_0	Element weight	Lognormal	$24\frac{kN}{m^3}$	0.04	-	-	[37]
g1	Surface dead load	Lognormal	$0.45\frac{kN}{m^2}$	0.04	-	-	[37]
q	Live load (kN/m2)	Eq. (22)	$0.5\frac{kN}{m^2}$	1.342	$\frac{1}{5}year^{-1}$	Service life	[37]

$$F_{q,max}(x) = exp\left[-\lambda\, T\left[1 - F_q(x)\right]\right] \tag{22}$$

Where $F_q(x)$ is the probability function of the sustained load, T is the reference exposition time and λ is the occurrence rate of sustained load changes. Thus, λT is the mean of the number of occupancy changes [37].

The parameters of the live load are defined in [36] depending on the user category. For this study, the values corresponding to sustained loads in office buildings have been selected, as they are representative of a large number of existing buildings.

Finally, γ_R is optimized through a least squares minimization of the average error between the reliability index (β) and the target reliability (β^*), in the design set:

$$e^2 = \frac{1}{n}\sum_{j=1}^{n}\left(\beta_j - \beta^*\right)^2 \tag{23}$$

The selection of the proper target reliability index (β^*) for structural assessment of existing structures is currently a subject of active research, Luechinguer and Fisher [38], Steenbergen et al. [11], Sýkora et al. [9]. As mentioned before, economic optimization can be used to derive target reliability values; however, human safety levels based on individual and societal risk should also be considered. As concluded in Steenbergen et al. [11], the minimum levels related to human safety are often critical target reliabilities for existing structures. Based on an analysis of the consequences to persons in more than 100 buildings collapses presented by Tanner and Hingorani [10] , Steenbergen et al. [11], these authors recommended a yearly target value of 4.2 (reference period T_{ref} = 1 year) for existing buildings, with a collapsed area, larger than 500 m^2 and in the consequence class CC2 according to EN 1990 [5].

Although the value of β_1^*= 4.7, for Tref = 1 year, is the one mostly accepted in new constructions; here, a range of possible target reliability indexes have been considered based on the recommendations of JCCS [37], depending on the cost of safety measures and consequences of failure (see Table 7). In this way, the sensitivity of the results to this target value can be also analysed. The reliability index for service life (T) different than 1 year can be computed by considering the probability of T successive non-failure years, and a rate of load changes λ. The reliability index is obtained as shown in Eq. (24).

Table 7. Recommended target yearly reliability indexes, β_1^* (adapted from JCCS [37])

	Consequences of failure		
Relative cost of safety measure	Minor	Moderate	Large
Large (A)	β_1^*= 3.1 ($P_{f,1}$≈10^{-3})	β_1^*= 3.3 ($P_{f,1}$≈5 10^{-4})	β_1^*= 3.7 ($P_{f,1}$≈10^{-4})
Normal (B)	β_1^*= 3.7 ($P_{f,1}$≈10^{-4})	β_1^*= 4.2 ($P_{f,1}$≈10^{-5})	β_1^*= 4.4 ($P_{f,1}$≈5 10^{-6})
Small (C)	β_1^*= 4.2 ($P_{f,1}$≈10^{-5})	β_1^*= 4.4 ($P_{f,1}$≈5 10^{-6})	β_1^*= 4.7 ($P_{f,1}$≈10^{-6})

$$\Phi\big(\beta(T)\big) = \Phi(\beta_1)^{\lambda T} \tag{24}$$

Similarly, the service life (remaining) of an assessed existing structure, or that of the designed strengthening may be different from that of a new construction. It may also be selected in terms of the planned future assessments and maintenance. Therefore, in this study the safety factor will be calibrated considering a range of different required service lives after the assessment. In this sense, the resulting factor will be useful for optimizing the possible combination of interventions.

4. RESULTS AND DISCUSSION

Figure 7 shows the least-square minimization for the case of one year exposition target reliability index of β_1^*=4.2, corresponding to the recommendations of Steenbergen et al. [11] for existing structures, and an expected remaining time in service of T=20 years. This is equivalent to a target reliability of 3.46 during the whole exposition period. By varying the shear safety factor used in design according to the resistance model of Section 2.1, the square of the difference between the calculated reliability index and the target one is minimized for a value of γ_R=1.124.

Similarly, the optimization of γ_R is carried out for the series of β_1^* of 3.3, 3.7, 4.2, 4.4 and 4.7, covering the range of recommended values for relative cost of safety measure for moderate and large consequences of failure. In addition, service life (T) is varied in the series of 5, 10, 20 and 50 years, for a total of 20 combinations. The shape of the resulting least-square optimization curves is similar to that in Fig. 7. Fig. 8 compares the target reliability index (β_1^*) for the different service life and the average reliability index ($\beta_{1,average}$) in the design set after optimization of the safety factor, for all the cases considered. It can be noticed that the correlation is good, with an average difference between the target and the average reliability index of 0.88%.

The optimized safety factors (γ_R) for each combination of β_1^* and T are shown in solid lines in Fig. 9. It can be observed that the effect of varying the service life is minor. This can be explained after analysing the influence of T in both the load and required reliability index. As shown in Eq. (23), larger exposition time implies a larger magnitude of the observed load with a given probability of not been exceeded. On the other hand, the target reliability index for a period range larger than one year, given by Eq. (24), reduces with time. Hence, the two effects compensate. The optimized values of γ_R can be approximated by Eq. (25). This approximation is represented in Fig. 9 as dotted lines.

$$\gamma_R = 0.237\beta_1^{1.09} \tag{25}$$

As can be observed, the range of values for the optimized safety factor is smaller than usually required for current shear resisting models and design codes. In particular, for target reliabilities of 4.4 and 4.7, comparable to new constructions, the shear safety factor varies between 1.17 and 1.28 for a service life of 50 years.

On the other hand, in assessing existing structures, smaller target reliability indexes can be justified, on the range of 3.3 and 3.7, based on larger cost of safety measure, as seen in Table 7. In these cases, γ_R can even take values between 0.83 and 1.0. However, these values are to be applied to the strength computed with the characteristic values of the material properties.

Fig. 10 shows the evolution of the reliability index with several design parameters, computed for each element of the design, for the case case $\beta_1^*=4.2$ and service life T=20 years. The shear safety factor obtained from Eq. (25) is $\gamma_R= 1.124$ and the target and average reliability indexes are shown in dashed red and green lines, respectively. The approximation of the average reliability to the target value is good, although some scatter is observed.

Fig. 10a shows the variation of the computed reliability as function of the live to dead load ratio (L/D). Most cases are distributed between 4.4 and 4.1, with a mean value close to the target value. However, two points show larger values of reliability, between 4.4 and 4.5 for L/D equal to 0.3. The influence of L/D seems to stabilize after L/D=0.6.

On the other hand, Fig. 10b, shows the same distribution when the effective ratio of transverse reinforcement varies. Reliability indexes are bigger in the region of zero or small transverse reinforcement ratio. Moreover, the two peak values identified in Fig. 10a lie within this region. This is explained as the elements not requiring transverse reinforcement, may resist larger shear force than the strictly demanded. For moderate and large shear reinforcement ratios, scatter of the computed reliability tends to a stable value of 4.15, only 2% smaller than the target value. The smallest observed index is 4.1, only 2.4% less than the target value.

Figs. 10c and 10d show the influence of the concrete strength and the effective depth. Besides the cases explained above, the scatter is reasonably independent of the concrete class. As for the effective depth, it seems to be a slight tendency to increase the reliability index for lager sections. However, the latter is correlated with the smaller transverse shear ratio in these points, as can be observed in Fig. 11b. Nevertheless, it should be highlighted that the model reliability index does not decrease for large size specimens, at least up to 1.2 m depth.

Fig. 11 shows the CoV of the computed reliability index of all cases, as computed during the calibration. It is evidenced that the scatter of the calibration increases for lower β_1, while it reaches an almost uniform value between 0.01 and 0.02 for $\beta_1>4$.

Alternatively, one may select a safety factor calibration that achieves a desired confidence level of the minimum reliability. In this case, the value of β_1 to be used in Eq. (26) may be increased to a value larger than the target, $\beta_{1,d} \geq \beta_1^*$. $\beta_{1,d}$ is defined so that it is guaranteed that 90% of the cases will show individual reliability indexes larger than a certain threshold of the target reliability index: $\beta_{1,individual} \geq c\, \beta_1^*$. Here, c is the fraction of the minimum reliability with respect to the target to be guaranteed. This is in agreement with Annex E of [7] if one considers that the value that guarantees a safe value 90% of the time is in line with the engineering judgement and tradition.

$\beta_{1,d}$ can be computed by multiplying the target reliability index (β_1^*) by a modification factor (f), as in Eq. (26). The proposed value for factor f is given in Eq. (27).

$$\beta_{1,d} = f\beta_1^* \tag{26}$$

$$f = \frac{\beta_{1,d}}{\beta_1^*} = 0.67 + 0.77c - 0.08\beta_1^* \geq 1 \tag{27}$$

In order to demonstrate the use of this approach in practice, consider the case of $\beta_1^*=3.3$, for a service life of 20 years. As observed in Table 7, this is equivalent to a moderate consequence of failure and large cost of safety measure. The safety factor for this mean reliability is, γ_R = 0.862. The reliability indexes for the individuals of the design set assessed with this safety factor are shown in Fig. 12a. The average reliability resulted as $\beta_{1,mean}$=3.416, which is larger than the target value. However, the smallest individual reliability index in the set is $\beta_{1,minn}$=3.050, which is 7.6% smaller than the target. Moreover, 34% of the set shows a computed reliability smaller than the intended one

Consider that it is desired to guarantee, with a 90% confidence, that the minimum reliability is larger than 0.85 of the target value, then Eq. (27) is used to obtain the modification factor as: $f = 0.67 + 0.77 \times 0.85 - 0.08 \times 3.3 = 1.06$. Therefore, the intended reliability index is $\beta_{1,d} = f\beta_1^* = 1.06 \times 3.3 = 3.50$. Further, the optimized shear safety factor will be computed from Eq. 26, as: $\gamma_{R,} = 0.23 \times 3.50^{1.09} = 0.928$.

The distribution of reliability indexes in the calibration with the latter safety factor ($\gamma_R = 0.928$) is shown in Fig. 12b. The mean computed reliability index in this case is 3.60 and the minimum value in the set is $3.34 > \beta_1^* = 3.3$. Hence, in this set there is no element with smaller reliability index than the target value ($\beta_1^* = 3.3$).

In order to show the effect of the model in design and assessment, the required shear reinforcement ratio in the design set according to the calibrated method, for yearly target reliabilities 4.7, 4.2 and 3.7, are compared against the current Eurocode and ACI-318 provisions. Note that the comparison with the ACI-318 is not direct, as the load factors are different from the ones used here for calibration. Moreover, the quantiles of the specified concrete strength also differ, so the relationship $f'_c \approx 1.05 f_{ck}$ was used.

Figure 13 shows the distribution of reinforcement ratio. When considering the target reliability of new design ($\beta^*_1=4.7$), the calibrated method prescribes, in average, higher reinforcement ratios than the Eurocode and ACI-318. Although, the percentage of elements falling in the region of small reinforcement ratios ($\rho_w f_{yd}$= 0 - 0.25 MPa) is similar to the Eurocode when considering $\beta^*_1=4.7$. However, in assessment, when lower reliability index can be justified, the percentage of elements with zero to small reinforcement ratio increases to almost 27% of the set, although it is still smaller than the share obtained for ACI-318 in this section. The average ratio for the three target reliabilities considered are 1.91 MPa, 1.36 MPa and 0.89 MPa, while the average ratios in the design set for the Eurocode and ACI-318 are 1.17 MPa and 1.29 MPa, respectively. In all cases, the maximum required reinforcement ratio was smaller than the needed in the Eurocode.

Further, the predicted strength for fixed reinforcement ratio and different target reliability index are compared to the code formulations in Table 8. The relative strength prediction increases as the target reliability is smaller. The percentage of elements predicted with larger strength than the code increases to 40% and to 80% in the case of Eurocode for β^*_1 equal to 4.2 and 3.7, respectively and from 60% to 77% in the case of ACI.

Finally, it should be taken into account that shear failure is, in general, brittle. In many design situations, when high ductility is required for correct performance, e.g. seismic situations, brittle failure modes can be prevented by applying "capacity design" approaches or over-strength factors in order to provide a larger safety margin to shear failure than bending. These approaches are also applicable with the present formulation. However, an advantage of the formulation is obtained from the fact that safety factors have been posed in terms of target reliability indexes. Hence, it allows for a reliability-based design in which, for example, a higher target reliability index can be attributed to shear failure than bending.

Although the model was derived from a mechanistic approach, the model error variable was calibrated with laboratory experimental data; and this data could not account for all realistic load conditions, such as those involving loads of long duration or repeated cyclic loading. However, this is a limitation of all shear design models used in practice today and present in the current design codes, as all them have been calibrated using laboratory experimental data as well. When more experimental data become available for other load situations, such as long-term or cyclic loads, the safety factor calibration may be updated accordingly.

Table 8. Representative values of the ratio of design shear strength of the calibrated model and the design strength of Eurocode and ACI-318 for different target reliability

$V_{Rd,model}$ / $V_{Rd,Code}$	β^*_1=4.7		β^*_1=4.2		β^*_1=3.7	
	EC-2	ACI-318	EC-2	ACI-318	EC-2	ACI-318
Maximum	1.23	3.50	1.65	3.58	2.01	3.66
Minimum	0.45	0.41	0.61	0.44	0.81	0.47
Average	0.75	1.00	0.97	1.15	1.26	1.38
CoV	0.26	0.46	0.25	0.40	0.22	0.37
% $V_{Rd,model} > V_{Rd,Code}$	13.0%	35.2%	39.8%	62.0%	81.4%	76.9%

5. CONCLUSIONS

A safety factor for the shear assessment of existing beams and slabs in existing buildings with reinforced concrete structures was calibrated. This was carried out using the shear resistance model published in [16], that is based on a multi-action principle and considers rational quantification of four simultaneous shear resisting mechanisms. The model was found to give the best approximation to a large database of shear tests, compared to modern design codes. In its present form, the model was developed for shear failure before yielding of longitudinal reinforcement.

This study has looked into different target values of safety as well as several remaining service life of the building under assessment. A wide range of reinforced concrete elements, with geometry and load conditions typical of building constructions was considered in the calibration of optimal safety factors for shear assessment. The covered sample included elements with and without shear reinforcement; therefore, the calibration is also suitable for both beams and slabs with live to dead load ratio (L/D) up to 0.8. The calibration is also adequate for normal and higher strength concrete, up to 90 MPa.

The safety factor proposed should only be used for the failure mode related to tension in the web and the compression chord capacity. It was not calibrated for crushing of concrete in thin webs.

It was found that the effect of the remaining service life (T) on the value of the optimized safety factor for shear strength can be neglected, compared to the effect of yearly target reliability index.

An analytical expression (Eq. 25) is proposed to compute the optimal safety factor for the considered model based on the adopted target reliability. The equation provides a very good fitting of the average reliability of the design set.

Adopting, for example, a yearly target reliability of 4.2, , suggested in [11] as appropriate for the assessment of existing structures, the corresponding safety factor obtained for the shear resisting model is 1.13, both for elements with and without transversal reinforcement. Other values of the safety factor can be derived using Eq. (25), if different target reliabilities are decided.

The shear resistance safety factor values of Eq. (25) are those that minimize the quadratic error between the reliability index of the investigated set and the target reliability value. The scatter of the observed reliability index ranged between CoV 2% and 9%, being larger for the smaller target reliability indexes. Hence, a fraction of the set may show less individual reliability indexes than the target. Therefore, a modification factor of the target reliability was proposed in Eq. (27), in order to guarantee a minimum individual reliability index with a confidence of 90%. For β^*_1=4.2, the application of this modification factor will modify the safety factor from 1.13 to 1.17 when considering the average reliability index or the guaranteed one.

The proposed shear safety factors have to be used jointly with the design equation as defined in Eq. (18) and the shear strength model as defined in Section 2. These safety factors are applicable to cases similar to those in the range of the sample analysed, which comprises a wide range of RC elements used in buildings. However, the proposed calibration methodology is general and may be applied to other shear strength models and other building floor systems. This approach will allow for quick and a more accurate assessment of existing reinforced concrete buildings to shear, and therefore, for lower costs of repair and strengthening, resulting on a more efficient allocation of limited resources, based on explicit target reliability indexes.

As shown in the paper, the model uncertainty is a strongly influent variable on the results derived from a calibration process. Therefore, the safety factors should be always considered to be valid for the particular case of the model used to obtain the design values of the variables. When deriving the parameters of the random variable model error, it is also of crucial importance to use, from the available experimental database, only those tests that correspond to the failure modes of interest. Failing to do that will derive on unreliable values of the safety factors.

It should be noticed that, although the model is derived from a mechanistic approach, the model error variable was calibrated with laboratory experimental data; and this data could not account for realistic load conditions that involve loads of long duration or repeated cyclic loading. However, this is a limitation of all shear design models used in practice today and present in the current design codes, as all them have been calibrated using laboratory experimental data as well.

ACKNOWLEDGEMENTS

This research was carried out with the support of the Spanish Ministry of Economy and Competitiveness and the European Regional Development Funds (ERFD), through the research projects BIA2012-36848, BIA2013-47290-R and BIA2015-64672-C4-1-R.

REFERENCES

[1] ACI-318-02 (2002), *“Building code requirements for structural concrete and commentary”*. Farmington Hills, MI. American Concrete Institute.

[2] ASCE/SEI-7 (2010), *“Minimum design loads for buildings and other structures”*, American Society of Civil Engineers, Virginia.

[3] EN1992 (2010), *“Eurocode 2: Design of concrete structures. Part 1: General rules and rules for buildings”*, European Committee for Standardization, Bruxelles.

[4] EN1991 (2003), *“Eurocode 1: Actions on structures. Part 1: General actions. Densities, imposed loads for buildings”*, European Committee for Standardization, Bruxelles.

[5] EN1990 (2002), “Eurocode 0: Basis of structural design. European Committee for Standardization, Bruxelles.

[6] ISO 13822 (2010). Basis for design of structures-Assessment of existing structures. Geneva, Switzerland.

[7] ISO 2394 (1998). General principles on reliability for structures. Second ed. Geneva, Switzerland.

[8] fib (2016), *“Partial factor methods for existing concrete structures”*, fib Bull. 80, Lausanne. ISBN 978-2-88394-120-5.
[9] Sýkora M, Diamantidis D, Holický M, Jung K (2016), “Target reliability for existing structures considering economic and societal aspects”, *Structure and Infrastructure Engineering*, doi: 10.1080/15732479.2016.1198394.
[10] Tanner P, Hingorani R (2015), “Acceptable risks to persons associated with building structures”, Structural Concrete, Vol 16, No. 3, 314-322
[11] Steenbergen R, Sýkora M, Diamantidis D, Holický M, Vrouwenvelder T (2015), “Economic and human reliability levels for existing structures”, Structural *Concrete*, Vol 16, No. 3, 323-332.
[12] Zwicky D, Vögel T (2000), *“Failure tests on dismantled prestressed concrete bridge girders”*, Zurich Institute of Structural Engineering IBK, Swiss Federal Institute of Technology ETH (*in German)*.
[13] Bergström M, Täljsten B, Carolin A (2009), “Failure load test of a CFRP strengthened railway bridge in Ömsköldsvik, Sweden”, *Journal of Bridge Engineering*, 14, 300-308.
[14] Ferreira D, Bairan JM, Mari (2013), “Assessment of prestressed concrete bridge girders with low shear reinforcement by means of a non-linear filament model”, *Structure and Infrastructure Engineering: Maintenance, Management, Life-Cycle and Performance,* DOI: 10.1080/15732479.2013.834944 .
[15] Ferreira D, Bairan JM, Marí A (2014), “Efficient 1D model for blind assessment of existing bridges: simulation of a full-scale loading test and comparison with higher order continuum models”, *Structure and Infrastructure Engineering: Maintenance, Management, Life-Cycle and Performance*, DOI: 10.1080/15732479.2014.964734.
[16] Marí A, Bairan JM, Cladera A, Oller E, Ribas C (2015), “Shear-flexural strength mechanical model for the design and assessment of reinforced concrete beams”, Structure and Infrastructure Engineering: Maintenance, Management, Life-Cycle and Performance, DOI: 10.1080/15732479.2014.964735.
[17] Bairan JM, Mari A (2007), “Multiaxial-coupled analysis of RC cross-sections subjected to combined forces”, *Engineering Structures*, 29, 1722-1738.
[18] Bairan JM, Mari A (2007), “Shear-bending-torsion interaction in structural concrete members: A nonlinear coupled sectional approach”, *Archives of Computational Methods in Engineering*, 14, 249-278.
[19] Carmona J., Ruiz G. (2014), “Bond and size effect of the shear capacity of RC beams without stirrups”, *Engineering Structures,* 66, 45-56.
[20] Yang Y. (2014), *“Shear behaviour of reinforced concrete members without shear reinforcement”*, Ph.D. Thesis, T.U. Delft, Delft.
[21] Kupfer H., Hilsdorf H., Rusch H (1969), “Behavior of concrete under biaxial stresses”, *ACI Journal*, 66 (8), 656-666.
[22] Zararis PD, Papadakis GC (2001), “Diagonal shear failure and size effect in RC beams without shear reinforcement”, *ASCE-Journal of Structural Eng.*, 127, 733-742. doi:10.1061/(ASCE)0733-9445(2001)127:7(733)
[23] Model Code (2012), *“Model Code 2010 – Final Draft”*, fib Bulletin 65 (Vol 1) and 66 (Vol 2) Switzerland.
[24] Collins MP, Bentz EC, Sherwood EG (2008), “Where is shear reinforcement required? Review of research results and design procedures”. *ACI Structural Journal*, 105, 590-600.
[25] Cladera A, Marí A (2007), “Shear strength in the new Eurocode 2. A step forward?”, *Structural Concrete*, 8, 57-66.

[26] Yu Q, Bazant ZP (2011), "Can stirrups suppress size effect on shear strength of RC beams?", *Journal of Structural Engineering*, 137, 607-617.

[27] Sykora M, Krejsa J, Mlcoch J, Prieto M, Tanner P (2018), "Uncertainty in shear resistance models of reinforced concrete beams according to *fib* MC2010", *Structural Concrete*, 19:284-295.

[28] Perez-Caldentey A, Padilla P, Muttoni A, Fernandez-Ruiz M (2012), "Effect of load distribution and variable depth on shear resistance beams without stirrups", *ACI Struct. J.*, V. 109, No. 5, 595-603.

[29] Kim J-C, Choi K-K (2017), "Laminated element analysis to predict the shear strength of concrete beams under distributed and concentrated loads", *Eng. Struct.*, 152, 45-46.

[30] Marí A, Cladera A, Bairan JM, Oller E, Ribas C (2014), "Shear-flexural strength mechanical model for the design and assessment of reinforced concrete beams subjected to point and distributed loads", *Front. Struct. Civ. Eng.*, 8(4), 337-353.

[31] Ellingwood B, Galambos T, MacGregor J, Cornell C (1980), "*Development of a Probablity Based Load Criterion for American National Standard A58*", U.S. Dept. of Commerce.

[32] Melchers RE (1987), "Structural reliability analysis and prediction", Ellis Horwood, England.

[33] Madsen HO, Krenk S, Lind NC (2006), *"Methods of structural safety"*, Dover New York.

[34] Casas JR (1997), "Reliability-based partial safety factors in cantilever construction of concrete bridges"¸ *ASCE-Journal of Structural Engineering*, 123 (3), 305-312

[35] Casas JR and Chambi JL (2014), "Partial safety factors for CFRP-wrapped bridge piers: Model assessment and calibration", *Composite Structures*, 118 (1), 267-283.

[36] Trentin C and Casas JR (2015), "Safety factors for GFRP strengthening in bending of reinforced concrete bridges", Composite Structures, 128, 188-198

[37] JCSS (2001), "*Probabilistic Model Code*", Joint Committee of Structural Safety, ISBN 978-3-909386-79-6.

[38] Luechinguer P, Fisher J (2015), *"New European technical rules for assessment and retrofit of existing structures"*, Report EUR27128 EN, Joint-Research Center, European commission.

FIGURE CAPTIONS

Figure 1. Basis of the distribution of shear stresses in shear capacity model

Figure 2. Stress envelopes, adapted from Kupfer et al. [21]

Figure 3. Parametric analysis for solution of compression chord shear capacity and comparison against linearized model (Eq. 7, in dashed lines)

Figure 4. Example of calculation of shear spans in the regions of a general beam

Figure 5. Static scheme of the elements in the design set, definition of the shear span length (*a*) and cross-section dimensions

Figure 6. Distribution of live to dead load ratio (L/D) in design set

Figure 7. Square error minimization for target $\beta_1^*=4.2$ and service life T=20 years

Figure 8. Correlation between average β corresponding to optimized γ_R and target values $\beta^*(T)$ for different combinations of annual target values β_1^* and service life periods (T) ranging from 5 to 50 years

Figure 9. Safety factor for different target β_1^* and service life. Eq. (26) shown in dashed lines

Figure 10. Distribution of β_1 for γ_{Rr} = 1.124, target $\beta_1^*=4.2$ and service life T=20 years with varying different design parameters

Figure 11. Variation of CoV of β_1 as function of mean value in the design set

Figure 12. Distribution of β_1 in the design set. a) γ_R= 0.862, for a mean target $\beta_1^*=3.3$, b) γ_R = 0.928, for a target $\beta_{1,d}=3.5$

Fig. 13 Distribution of the shear reinforcement ratio designed for different β_1^*, Eurocode and ACI-318

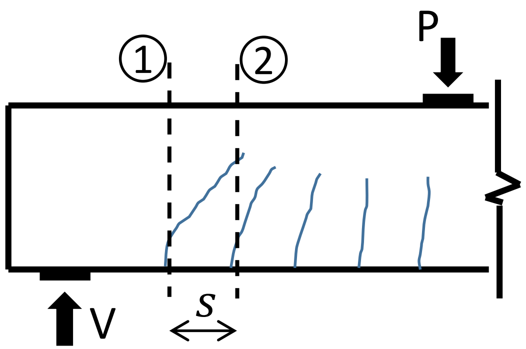

a) Free body cut limited by cross-sections 1 and 2

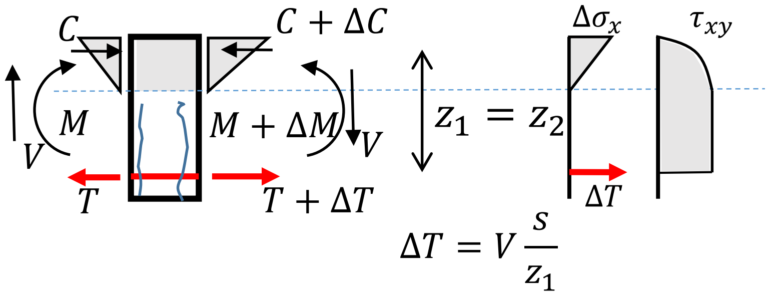

b) Free body equilibrium and stress distribution for perfect beam-action

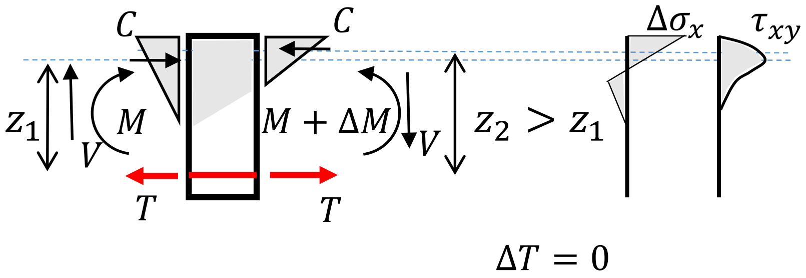

c) Free body equilibrium and stress distribution for perfect arch-action

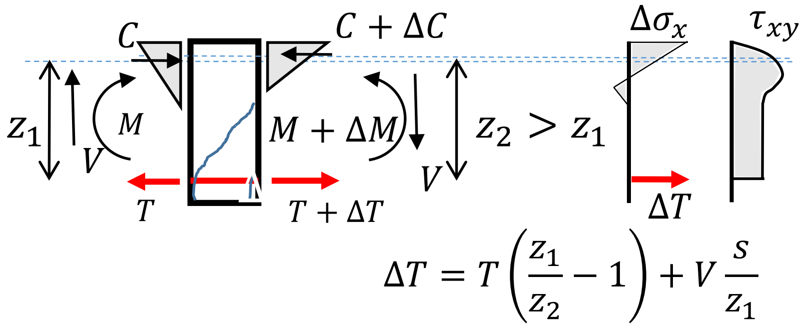

d) Free body equilibrium and stress distribution for combined beam-arch action

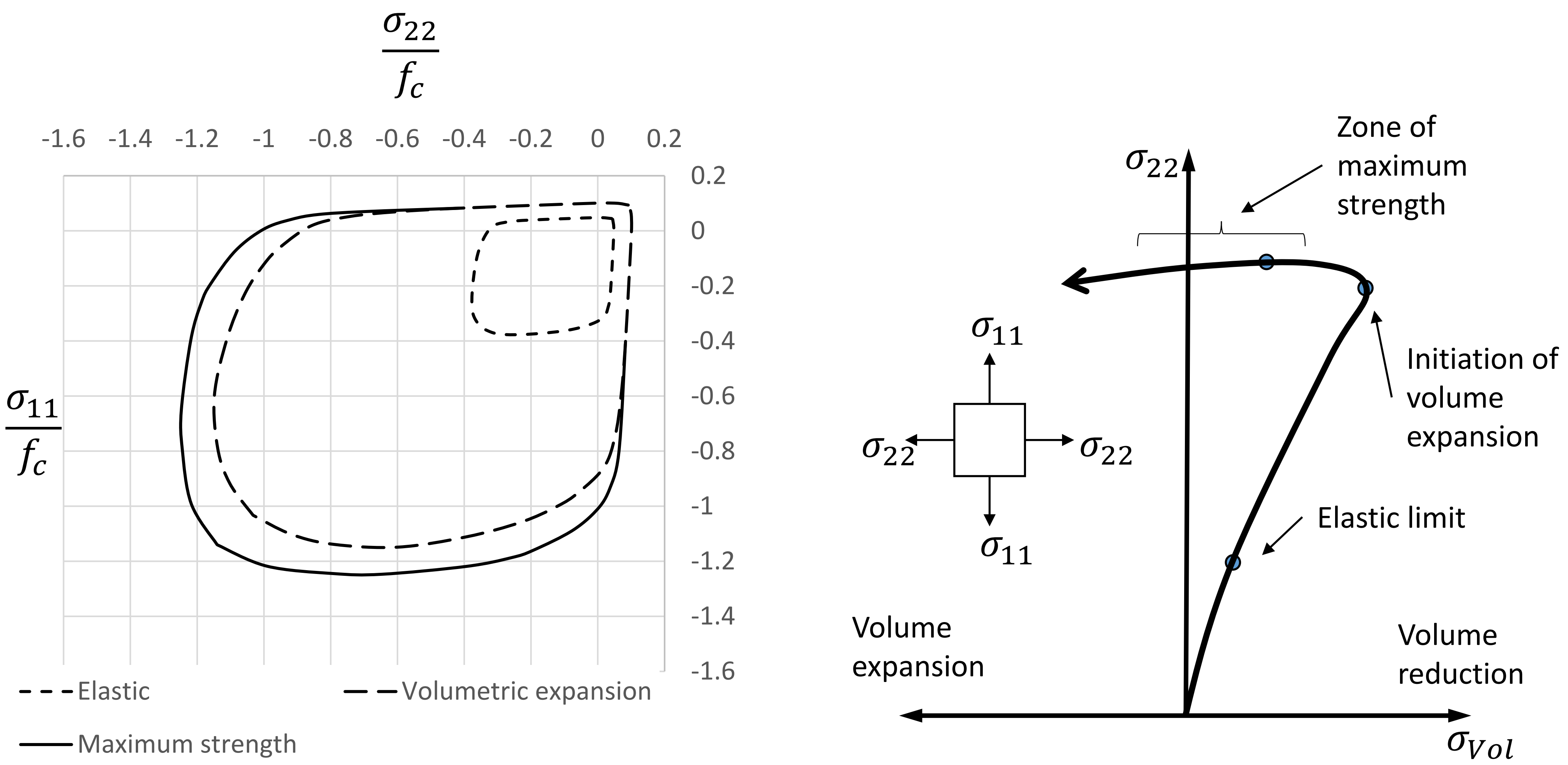

$\frac{\sigma_{22}}{f_c}$
-1.6 -1.4 -1.2 -1 -0.8 -0.6 -0.4 -0.2 0 0.2
0.2 0 -0.2 -0.4 -0.6 -0.8 -1 -1.2 -1.4 -1.6
$\frac{\sigma_{11}}{f_c}$
Elastic
Volumetric expansion
Maximum strength
Zone of maximum strength
σ_{22}
σ_{11}
σ_{22}
σ_{22}
σ_{11}
Initiation of volume expansion
Elastic limit
Volume expansion
Volume reduction
σ_{Vol}

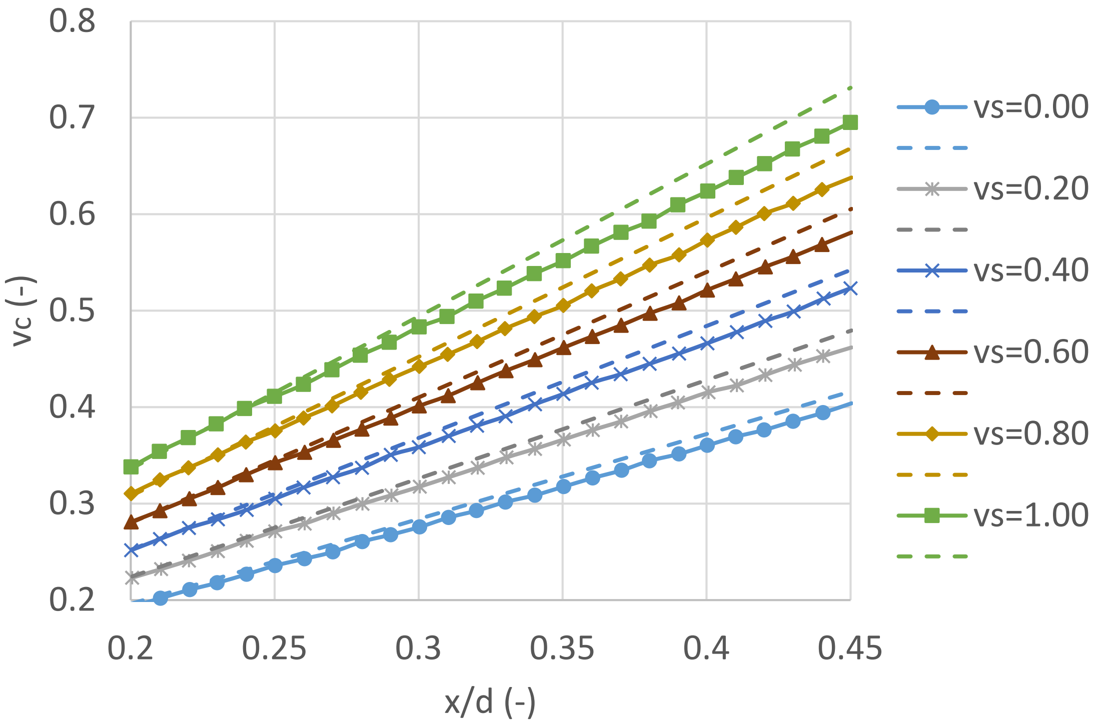

0.8
0.7
0.6
0.5
0.4
0.3
0.2
vc (-)
0.2
0.25
0.3
0.35
0.4
0.45
x/d (-)
vs=0.00
vs=0.20
vs=0.40
vs=0.60
vs=0.80
vs=1.00

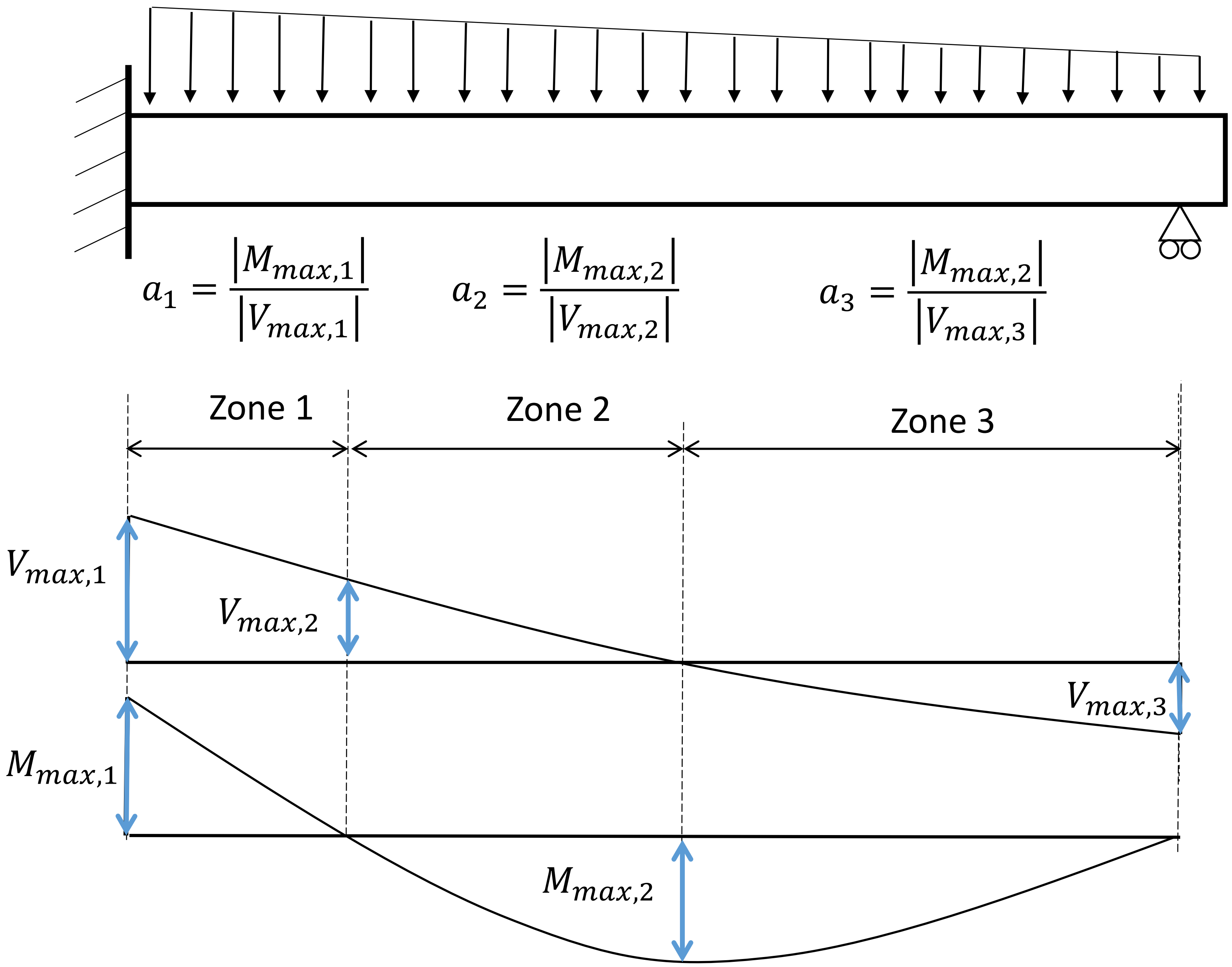

$a_1 = \frac{|M_{max,1}|}{|V_{max,1}|}$
$a_2 = \frac{|M_{max,2}|}{|V_{max,2}|}$
$a_3 = \frac{|M_{max,2}|}{|V_{max,3}|}$
Zone 1
Zone 2
Zone 3
$V_{max,1}$
$V_{max,2}$
$V_{max,3}$
$M_{max,1}$
$M_{max,2}$

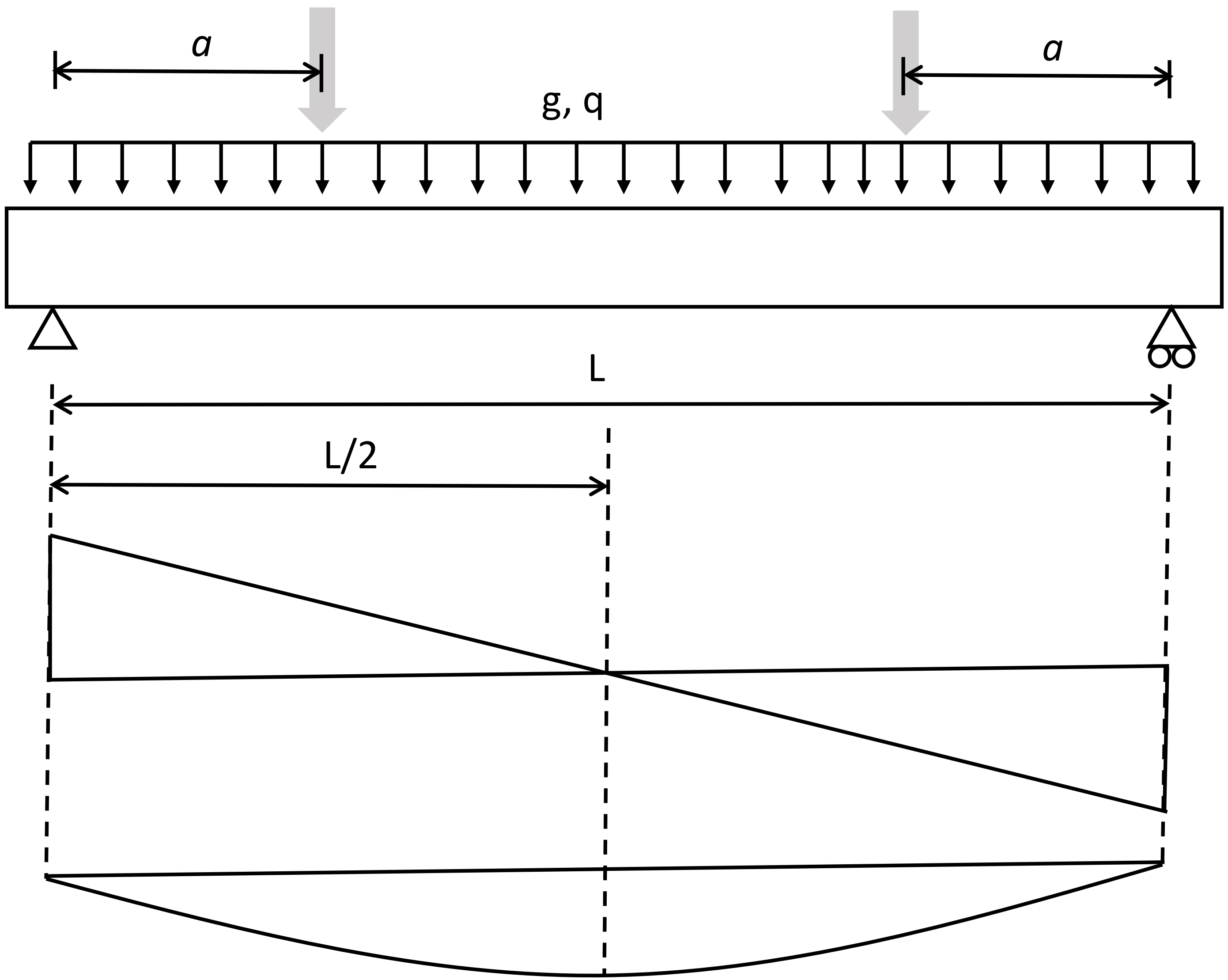

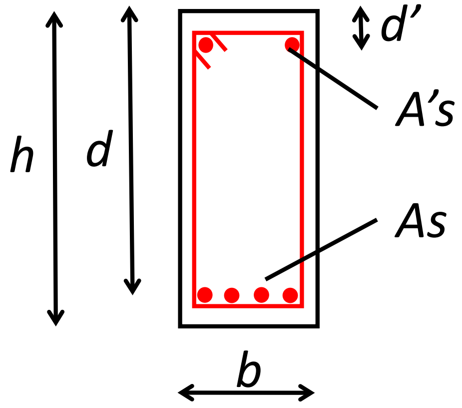

$$a = \frac{M_{max,shear\ span}}{V_{max,shear\ span}} = \frac{L}{4}$$

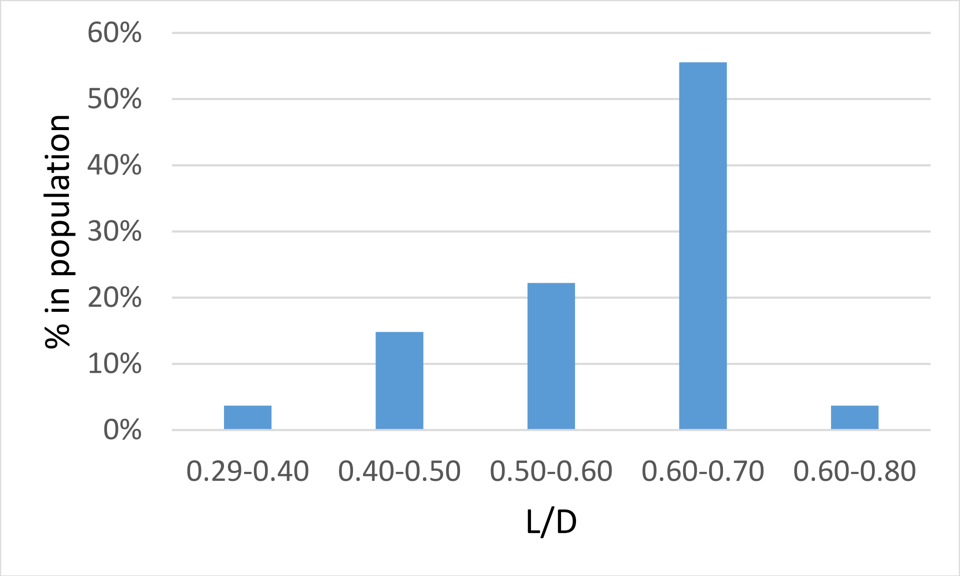

60%
50%
40%
30%
20%
10%
0%
% in population
0.29-0.40
0.40-0.50
0.50-0.60
0.60-0.70
0.60-0.80
L/D

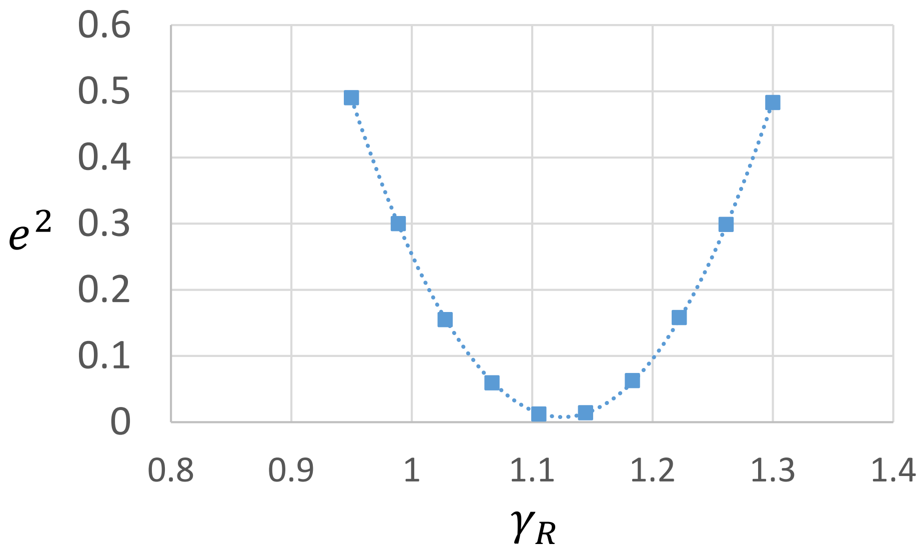

0.6
0.5
0.4
0.3
0.2
0.1
0
e^2
0.8
0.9
1
1.1
1.2
1.3
1.4
γ_R

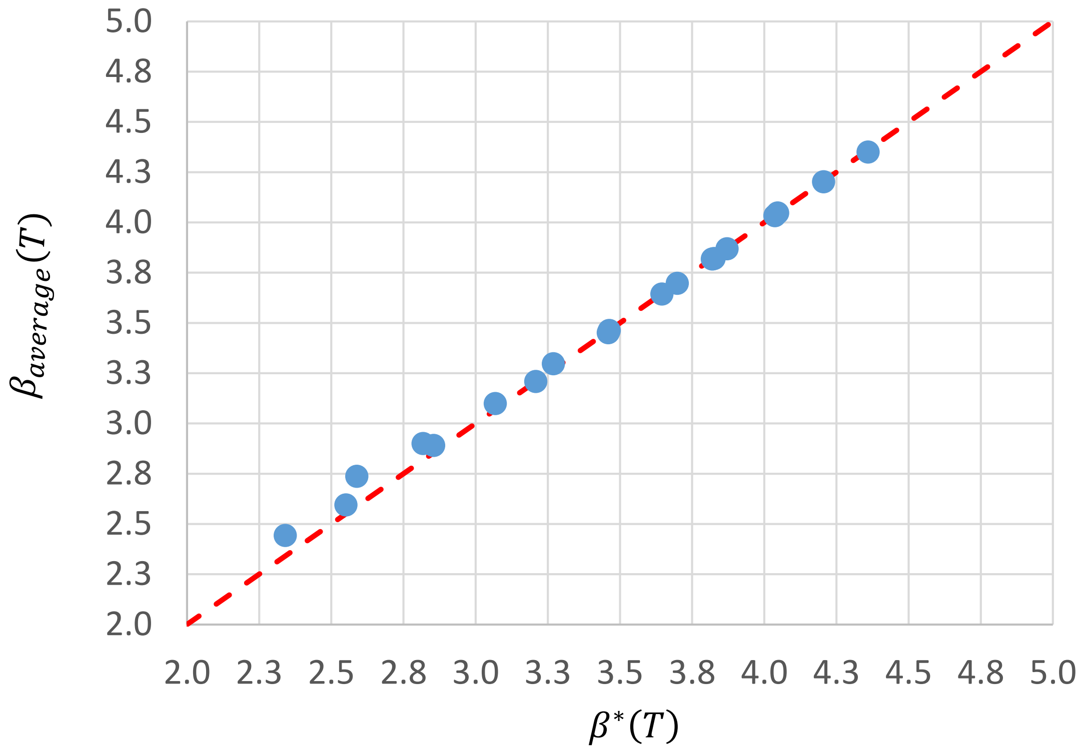
5.0
4.8
4.5
4.3
4.0
3.8
3.5
3.3
3.0
2.8
2.5
2.3
2.0
$\beta_{average}(T)$
2.0 2.3 2.5 2.8 3.0 3.3 3.5 3.8 4.0 4.3 4.5 4.8 5.0
$\beta^*(T)$

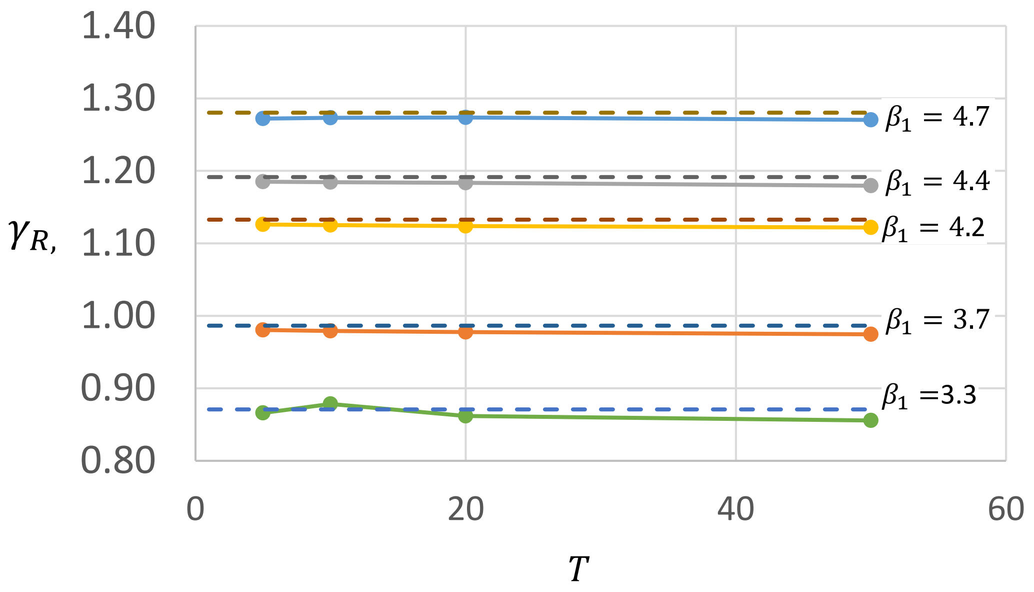

1.40
1.30
1.20
1.10
1.00
0.90
0.80
$\gamma_{R,}$
0
20
40
60
T
β_1 = 4.7
β_1 = 4.4
β_1 = 4.2
β_1 = 3.7
β_1 =3.3

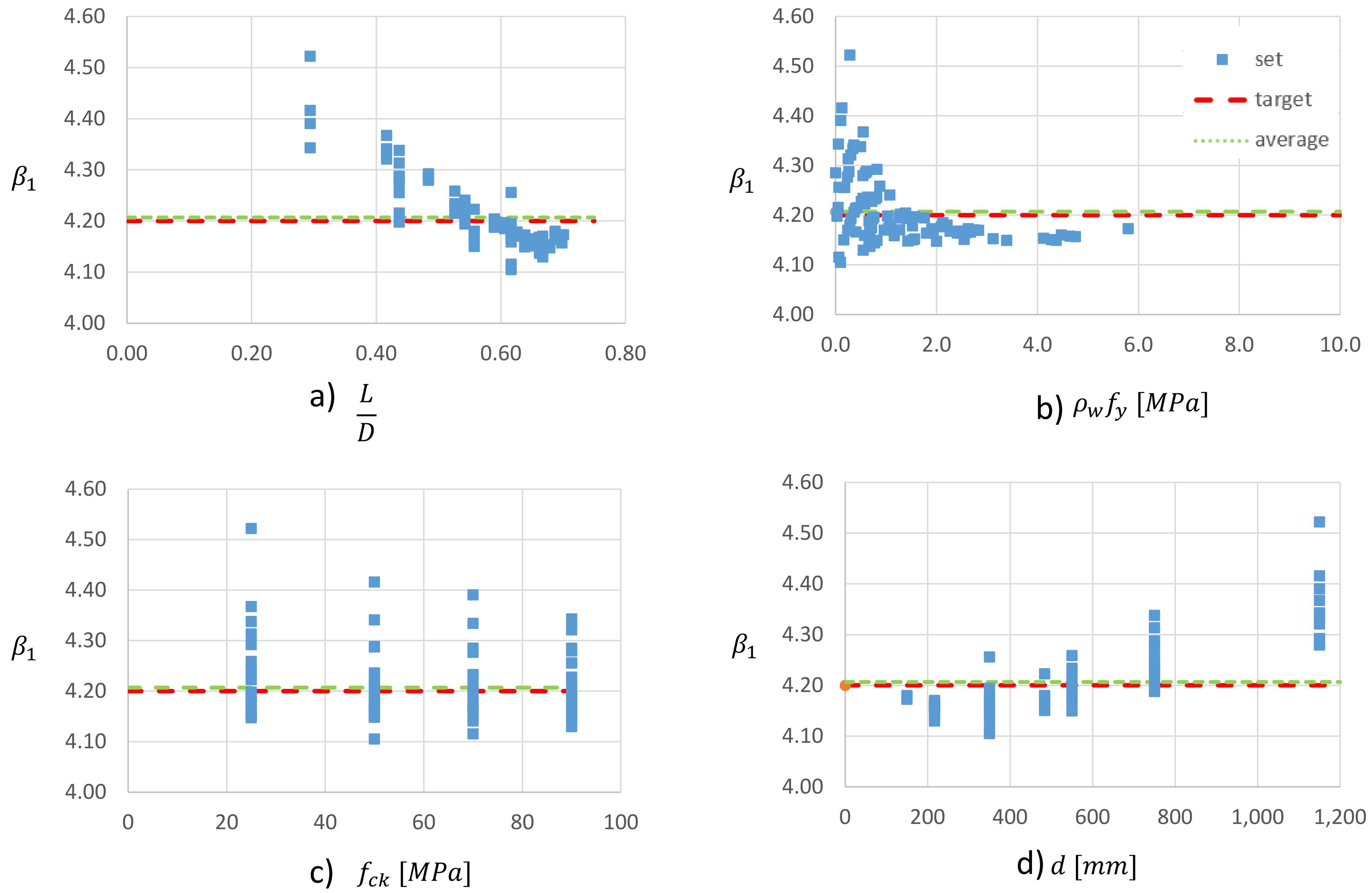

4.60
4.50
4.40
4.30
4.20
4.10
4.00
β_1
0.00
0.20
0.40
0.60
0.80
a) $\frac{L}{D}$
set
target
average
0.0
2.0
4.0
6.0
8.0
10.0
b) $\rho_w f_y$ $[MPa]$
0
20
40
60
80
100
c) f_{ck} $[MPa]$
0
200
400
600
800
1,000
1,200
d) d $[mm]$

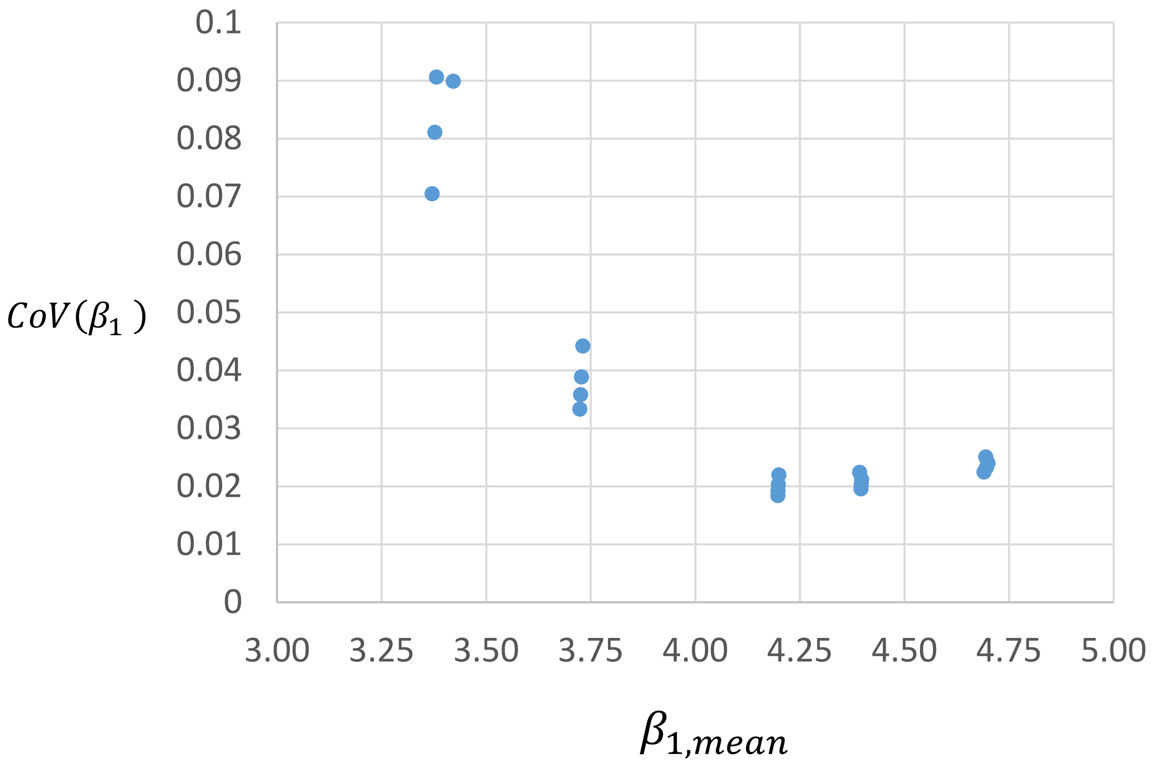
CoV(β1)
0.1
0.09
0.08
0.07
0.06
0.05
0.04
0.03
0.02
0.01
0
3.00
3.25
3.50
3.75
4.00
4.25
4.50
4.75
5.00
β1,mean

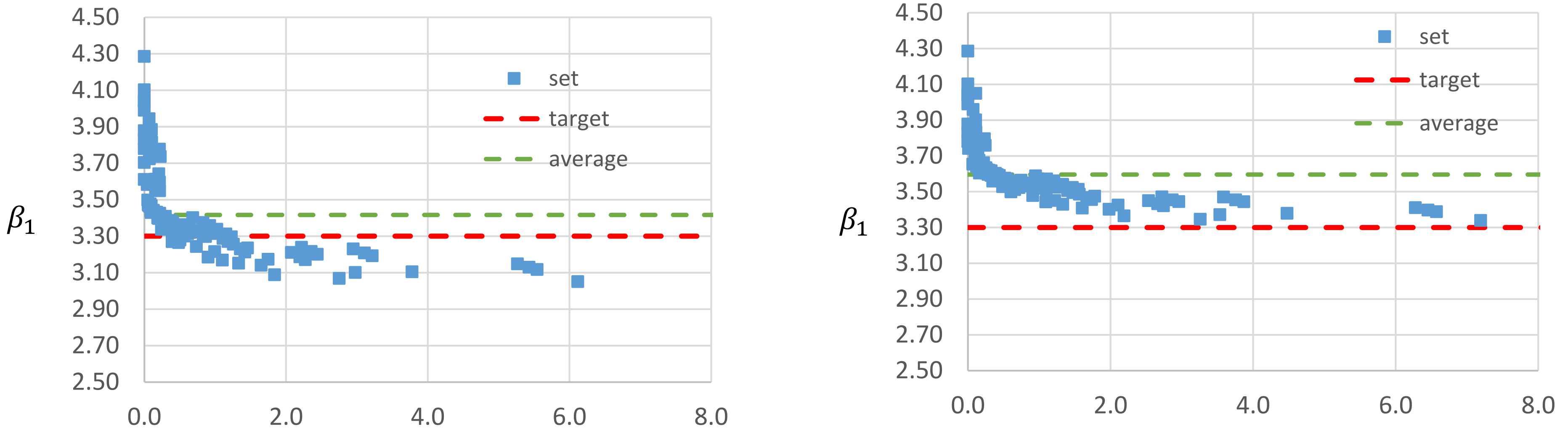

a) $\rho_w f_y$ $[MPa]$

b) $\rho_w f_y$ $[MPa]$

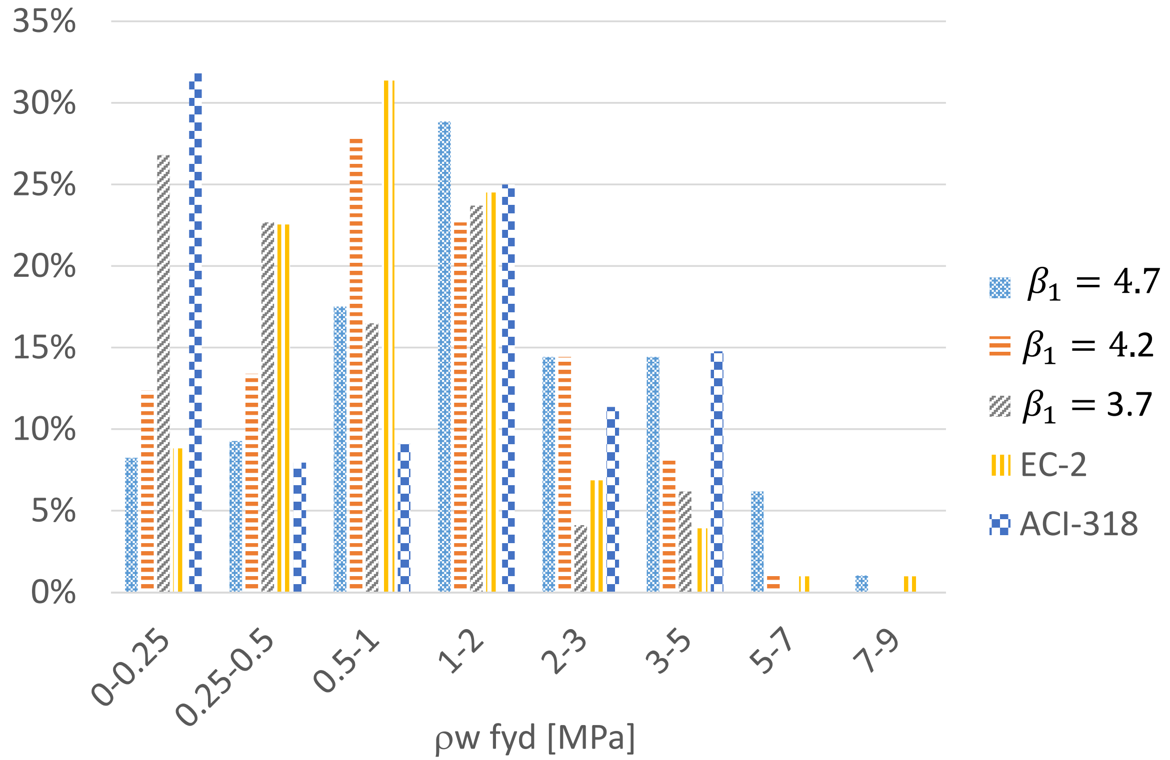

35%
30%
25%
20%
15%
10%
5%
0%
0-0.25
0.25-0.5
0.5-1
1-2
2-3
3-5
5-7
7-9
ρw fyd [MPa]
$\beta_1 = 4.7$
$\beta_1 = 4.2$
$\beta_1 = 3.7$
EC-2
ACI-318